

Characterization of 12-8-diacetylene Langmuir-Blodgett films by scanning-force microscopy

Hemasiri Vithana,¹ David Johnson,¹ Raymond Shih,² and J. Adin Mann, Jr.²

¹Liquid Crystal Institute and Department of Physics, Kent State University, Kent, Ohio 44242

²Department of Chemical Engineering, Case Western Reserve University, Cleveland, Ohio 44106

(Received 23 December 1993; revised manuscript received 1 July 1994)

Multilayers of 12-8-diacetylene (10,12-pentacosadiynoic acid) films prepared by the Langmuir-Blodgett technique on ordinary microscope and indium tin oxide coated glass were characterized by scanning-force microscopy (SFM) before and after polymerization. Well-resolved molecular images were obtained in monomeric diacetylene films over areas as large as $60 \times 60 \text{ nm}^2$. After exposing the films to uv radiation for polymerization it was found that the layer thickness decreased by approximately 10% while lattice parameters changed nearly by 5%. Also it was found that the roughness increased upon polymerization and the molecular scale images were better resolved in one lattice direction than in the other. The better resolved direction may be the polymer backbone of the film suggesting that the force between the SFM tip and the sample is strong enough to penetrate through the C_{12} -alkyl chains without seriously damaging the film.

PACS number(s): 61.16.Ch, 68.18.+p

INTRODUCTION

The Langmuir-Blodgett (LB) technique can be utilized to prepare well ordered single-layer (monolayer) and multilayer films of amphiphilic organic materials. In this technique a monolayer is prepared at the air-water interface to a specified surface pressure-area state and transferred to various substrates. By repeating this process it is possible to form multilayer films. Many kinds of amphiphilic materials have been found to form LB films, leading to a wide range of application areas such as microelectronics, nonlinear optics, cell membrane models, and biosensors [1]. For all these applications it is usually necessary to have defect free uniform films, and therefore the quality and structure of the films must be evaluated at high resolution. For this purpose several techniques such as x-ray diffraction [2-4], electron diffraction [5,6] and various spectroscopies [7-10] have been used. All these techniques give information averaged over areas of square millimeters. With the invention of scanning-force microscopy [11] it has become possible to study films at molecular resolution [12-15] and to detect local defects on the scale of nanometers [16]. In order to use scanning tunneling microscopy (STM) for surface studies, the surface has to be conductive. In the case of insulating surfaces like LB films, the technique is limited to thin layers deposited on a conducting surface such as graphite or coated with a thin layer of conducting material like platinum. However, Guckenberger *et al.* [17] studied uncoated purple membranes using STM with tunneling currents less than 1 pA and tunneling voltages above 7 V. They observed both positive and negative contrast in their images, and the measured thickness of the membrane ranged from 3.5 to 10 nm, depending on the contrast. Specht, Ohnesorge, and Heckl [18] observed tunneling currents through organic thin films deposited on graphite 30 Å thick at bias voltages $\approx 1 \text{ V}$ and through films 100 Å thick at higher negative bias voltages $\approx 6 \text{ V}$. Although

the scanning-force microscope (SFM) is a nearly ideal tool for the study of molecular scale topography of LB films of any thickness deposited on any kind of substrate, the fact is that the SFM may image artifacts resulting from the probe tip plowing through the relatively soft material that forms LB multilayers. Indeed, the problem of artifacts intruding in the interpretation of SFM images has been described recently by Ohnesorge and Binnig [19]. Their recipe for obtaining point accurate images at atomic resolution involves operating at forces less than a nanonewton. Gaub [20] also described the artifact problem with emphasis on soft films such as LB structures, and was rather optimistic about images made in the usual force range of a few nanonewtons. We are well aware of these problems, and will show that defects which appear to be dislocations can be found regardless of the orientation of the sample with respect to the scan direction.

Among the various kinds of organic materials which can form LB films, polymerized fatty acids such as diacetylenic fatty acids have attracted considerable attention [1]. These materials have two conjugated triple bonds per molecule, and can be polymerized to form a polydiacetylenic bond hence giving more rigidity to the film. Polydiacetylenic films have strong third-order optical susceptibility and anisotropic electrical conductivity which have been investigated in detail [21,22]. LB films prepared from diacetylene derivatives have been investigated by SFM [23-26], fluorescence microscopy [24-27], x-ray diffraction [3,4,7,28], electron diffraction, optical microscopy [29,30], ellipsometry, and Fourier transform infrared [9].

In this paper we report the SFM characterization of 12-8 monomeric $[(\text{CH}_3-(\text{CH}_2)_{11}-\text{C}\equiv\text{C}-\text{C}\equiv\text{C}-(\text{CH}_2)_8-\text{COOH}]$ and polymeric diacetylene LB films of various numbers of layers deposited on ordinary microscope glass or on indium tin oxide (ITO)-coated glass. Although the substrates were not atomically smooth, we were able to obtain molecular-resolved images in all

monomer and polymer films, and the polymer backbone was also resolved in polymerized films.

EXPERIMENT

A 12-8-diacetylene monomer was synthesized by the method of Walsh [31]. Preparation of LB films was carried out in a class 100 clean room at a temperature of $20 \pm 1^\circ\text{C}$ on a Lauda Teflon coated LB balance with trough dimension of $70 \times 15 \times 0.6 \text{ cm}^3$. An aqueous solution of 10^{-3} M CdCl_2 in pure water (Millipore) was used as the subphase. The pH was adjusted to 7 with NaOH, and the subphase was kept at room temperature. Substrates used were ordinary microscope glass and ITO coated glass (Donnelly Corp., MI) with rms roughnesses of 0.65 and 0.42 nm, respectively, over an area of $500 \times 500 \text{ nm}^2$ as measured by SFM. These substrates were carefully cleaned prior to the film deposition, first with distilled water and detergent (Alconox) and then placed in a chromerge cleaning solution (for preparing chromic sulfuric acid solutions) (Fisher Scientific) bath and agitated (ultrasonicator) for 15 min. Subsequently the substrate was rinsed thoroughly with distilled water and baked at 110°C for 1 h.

The 12-8-diacetylene monomer was spread on the subphase from chloroform solution. After leaving the lid of the trough open for about 5 min for solvent evaporation, the film was compressed at a rate of 2 cm/min from a surface area of $0.6\text{--}0.2 \text{ nm}^2/\text{molecule}$. Pressure-area isotherms of diacetylene monolayers on the subphase at room temperature are shown in Fig. 1. Our experiments were all done at $\text{pH}=7$. Y type samples where head-to-head and tail-to-tail packing orders of the diacetylene molecules were deposited at point A ($0.2 \text{ nm}^2/\text{molecule}$), which is shown in Fig. 1. Dipping was initiated after waiting for 30 min at a surface pressure of 30 mN/m. Substrates were moved vertically through the diacetylene monolayer at a speed of 2 mm/min. We found that except for the first dip the transfer ratio was nearly 100%. Polymerization was initiated after transferring the film to the substrate by exposing it to unpolarized uv radiation ($\lambda=254 \text{ nm}$, $420 \mu\text{W}/\text{cm}^2$ at 15 cm) for 30 min. Note that the monolayer must be well ordered for polymerization to occur to any extent.

SFM measurements were carried out in air at room

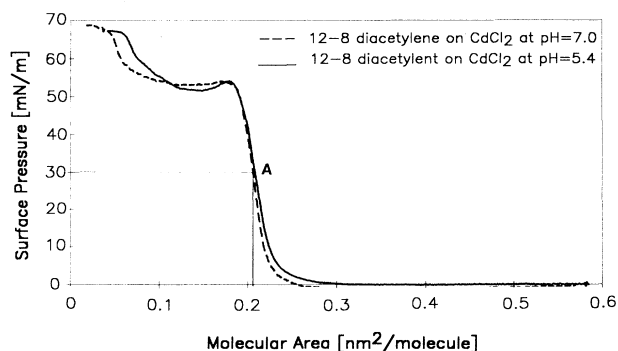


FIG. 1. Pressure-area isotherms for 12-8-diacetylene molecules at different pH values and at 20°C .

temperature on a vibration isolation stage using a Digital Instrument Nanoscope III. For large scans the D head (maximum scan size $12 \times 12 \mu\text{m}^2$) was used while for small scans the A head (maximum scan size $0.7 \times 0.7 \mu\text{m}^2$) was used. Cantilevers used have a pyramidal silicon nitride tip (Park Scientific Instruments) with a spring constant of $\sim 0.06 \text{ N/m}$. For all our scans forces between the sample and the tip were less than 10^{-8} N . The SFM was used in the deflection mode (best molecular resolved images were obtained in this mode) where the sample is held at a constant height z and the cantilever deflection is monitored during the X-Y scan. To verify the images, samples were scanned at several locations and also in more than one direction to establish repeatability. For molecular-resolved images, scanning speeds of 61 Hz with 512×512 points and 110 Hz with 256×256 points were used. After scanning for about 5 min at the same position all noticeable shifts gradually decreased and disappeared, and the images were subsequently captured. To reduce the high-frequency spatial noise in the images a 3×3 low pass numerical filter was applied once to all the molecular level images presented here except where indicated. In each molecular level image, the inset gives the schematic of the lattice (not in scale) oriented as in the image.

RESULTS AND DISCUSSION

Figure 2(a) shows the surface of the film obtained after completion of one dipping cycle through the diacetylene monolayer; a microscope glass slide was the substrate. Spikes appearing in this image could be artifacts due to dust particles. As can be seen, this is not a complete deposition. Islandlike features are evident ranging in size up to $5.0 \mu\text{m}$ in diameter. The height of these islands is $8.84 \pm 0.6 \text{ nm}$, consistent with a three-layer film. The maximum length of the 12-8-diacetylene molecule was calculated by computer modeling assuming standard bond lengths and angles and found to be 2.96 nm. The lowest level of Fig. 2(a) was scanned separately and has a rms roughness of 0.58 nm in an area of $500 \times 500 \text{ nm}^2$, which is close to the measured average rms roughness of the substrate (0.65 nm). Further evidence that this is indeed the bare substrate is that high force scans did not alter the surface topography of these regions. The failure to achieve monolayer coverage could have several origins. If there are impurities on the substrate or if it is chemically and/or structurally heterogeneous, which is likely, or if the diacetylene material has some impurities in it, the film may not uniformly adhere to the substrate surface at the first dip. Surface roughness may also play a role in reducing the wettability of the substrate. If for any reason there exists a random distribution of regions where the monolayers stick to the substrate, the film stress, which may be fairly uniform on the trough, may become highly nonuniform on the substrate leading to randomly distributed breaks in the film followed by a folding up of the free (unstuck) portions of the film into a bilayer and redeposition onto the strongly bound monolayer islands to form the three-layer islands observed. We were able to obtain images with molecular resolution from islands that may have formed by this mechanism.

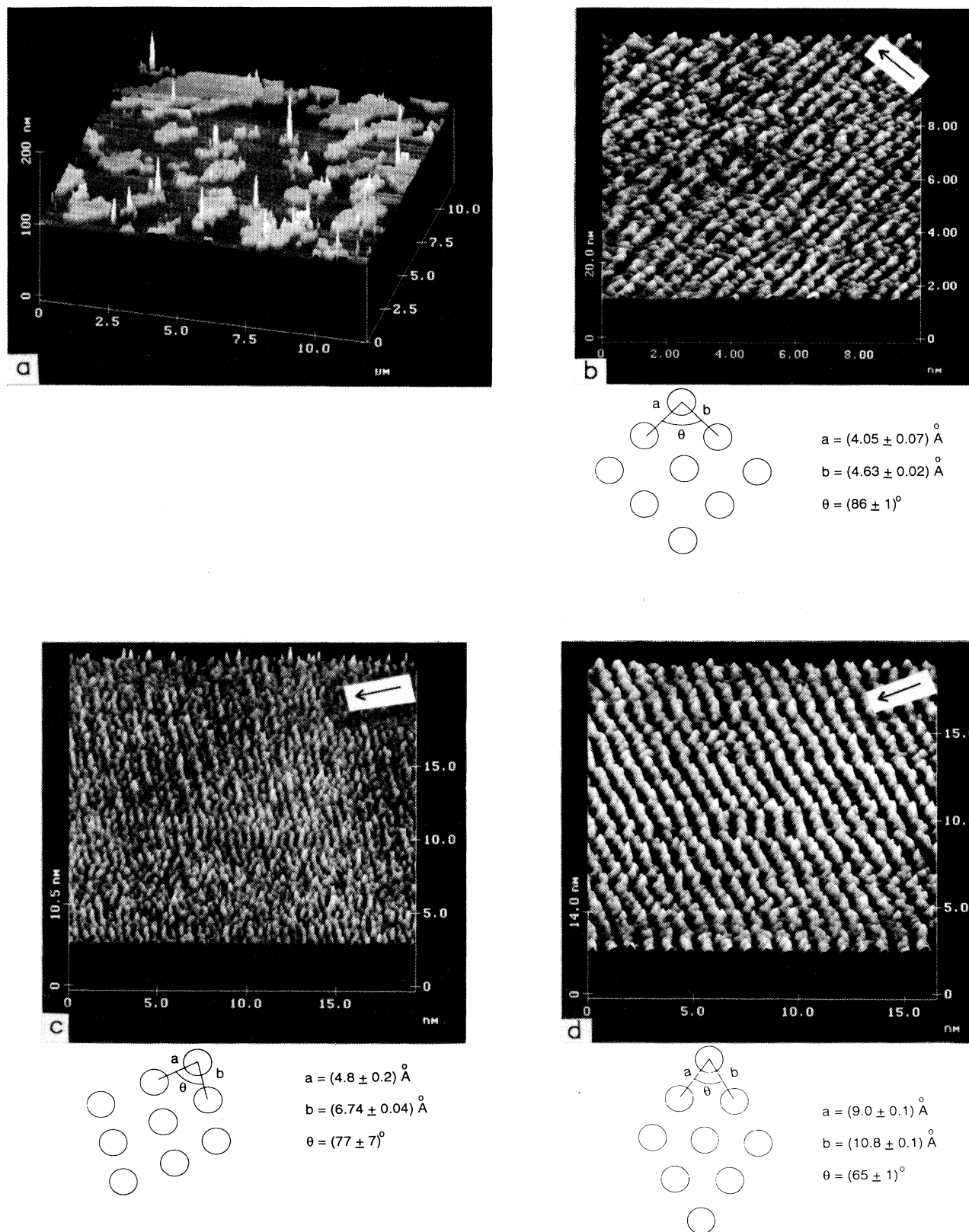


FIG. 2. (a) $12 \times 12\text{-}\mu\text{m}^2$ SFM image of the surface obtained after completion of one cycle through the diacetylene monolayer. (b)–(d) Molecular-resolved SFM images with the lattice structures obtained on three different islands. Arrow indicates the direction of dipping.

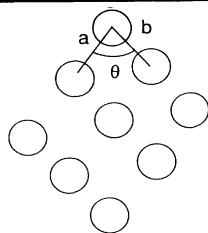
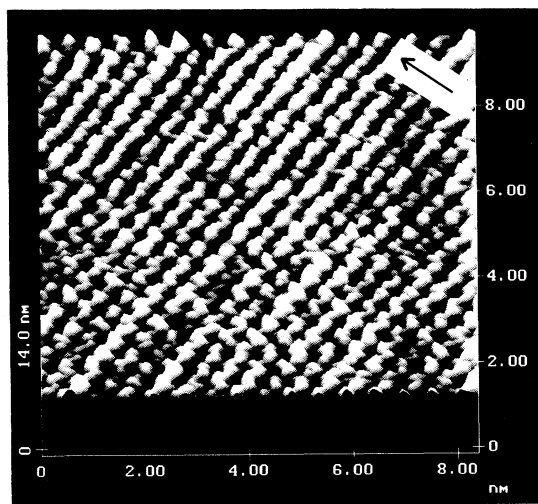
TABLE I. Lattice parameters of the diacetylene LB films (polymeric and monomeric) with different numbers of layers.

| No. of layers | Type | Figure No. | a (Å) | b (Å) | Θ° |
|---------------|---------|------------|-----------------|-----------------|----------------|
| 3 | monomer | 2(b) | 4.05 ± 0.07 | 4.63 ± 0.02 | 86 ± 1 |
| 3 | monomer | 2(c) | 4.75 ± 0.15 | 6.74 ± 0.04 | 77 ± 7 |
| 3 | monomer | 2(d) | 9.0 ± 0.1 | 10.8 ± 0.1 | 65 ± 1 |
| 9 | monomer | | 4.21 ± 0.13 | 4.71 ± 0.25 | 71 ± 7 |
| 15 | monomer | | 4.54 ± 0.25 | 4.91 ± 0.25 | 71 ± 3 |
| 9 | polymer | | 4.68 ± 0.12 | 5.57 ± 0.2 | 102 ± 6 |

Figures 2(b)–2(d) show three images of different sizes. These images were obtained from three different islands on the film. We found that although the molecules are arranged in an orderly fashion, the lattice parameters vary from island to island. Also within an island, lattice parameters were found to vary from place to place, and this variation as well as the island to island variations were larger for smaller islands. Lattice parameters were deduced from the two-dimensional fast Fourier Transformed filtered images of the SFM data calibrated against mica and are given in Table I. Long term scanning even with small forces ($< 10^{-8}$ N) can cause a large mechanical deformation on small islands and could cause the observed differences in the lattice parameters. It is also observed that scanning for approximately 1 min with a high force (7×10^{-8} N) brushed off these islands, indicating, as expected, that the film is not rigidly bound to the substrate. Variation in substrate topography and

chemistry are also candidates for lattice parameter variations.

Figure 3 shows a molecular resolved image obtained from a continuous nine-layer film deposited on microscope glass. Variation of lattice parameters from place to place were negligible by comparison with the previous film, indicating that this film is much more uniform and well ordered. Figure 4 shows an image from a 15-layer film, the lattice parameters are also consistent from place to place. Some areas of the film were less well resolved than others, which could be due to the roughness of the underlying substrate or defects of the film itself (Fig. 4, upper part). We were able to obtain molecular resolved images in areas as large as $60 \times 60 \text{ nm}^2$, which is near the limit of molecular resolution of 512×512 pixel scans. Continuously ordered regions appeared to exist on the scale of micrometers but micrometer sized scans could

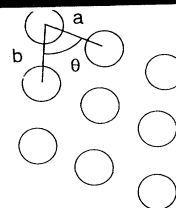
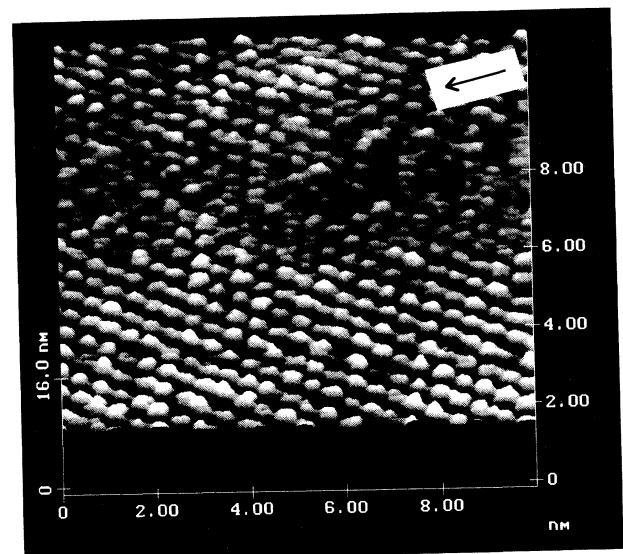


$$a = (4.34 \pm 0.02) \text{ \AA}$$

$$b = (4.49 \pm 0.05) \text{ \AA}$$

$$\theta = (76 \pm 1)^\circ$$

FIG. 3. Image with molecular resolution of a nine-layer film with the lattice structure. The arrow indicates the direction of dipping.



$$a = (4.65 \pm 0.08) \text{ \AA}$$

$$b = (4.81 \pm 0.03) \text{ \AA}$$

$$\theta = (71 \pm 2)^\circ$$

FIG. 4. Image with molecular resolution of a 15-layer film with the lattice structure. The arrow indicates the direction of dipping.

not resolve molecules. Long wavelength random undulations (amplitudes ranging up to ~ 35 nm) of the film were visible in these images. However, we did not observe any noticeable variations in lattice parameters from the top of the hills to the valleys of these undulations. In both the nine- and 15-layer films these long wavelength (~ 150 nm) height variations were visible in large scans ($10 \times 10 \mu^2$) and could arise from the nonuniform initial deposition shown in Fig. 2(a).

Table I shows the average values of the lattice parameters obtained over several images of the nine- and 15-

layer films. These values, except from the three-layer films, are in agreement with previous work on 12-8-diacetylene by electron diffraction on multilayers [7] and SFM measurements in an aqueous environment on monolayer films [26]. Even though the substrates and first monolayer (composed of three-layer islands) were not atomically smooth, we were able to obtain good molecular resolved images in air of all LB films. This result indicates that molecular resolution of amphiphilic materials is possible on relatively rough amorphous surfaces, although true monolayers on rough surfaces have yet to be

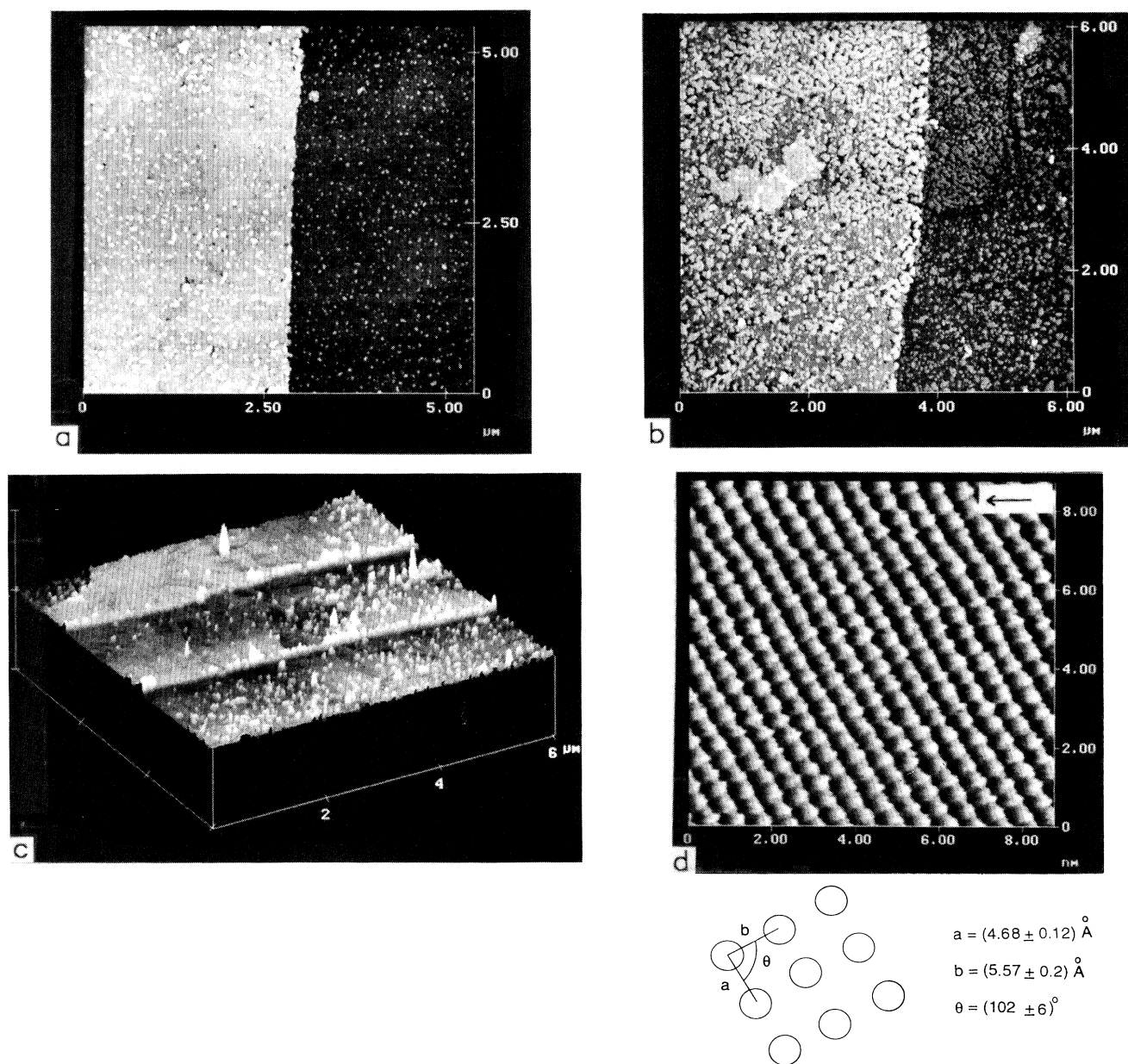


FIG. 5. (a) Image of a bilayer step deposited on a 9/11 layer film on ITO glass. (b) Image of the different position of the same step as in (a) after exposure to uv radiation for 30 min. (c) Image of three bilayer steps; 9/11/13 layers deposited on ITO glass. (d) 12.5×12.5 -nm² image with molecular resolution of a nine-layer polymerized film with the lattice structure. The arrow indicates the direction of dipping.

studied. Previous results on fatty acids at molecular resolution have been obtained by SFM only by using atomically flat surfaces such as polished silicon wafers, mica, etc. [26,32].

Figure 5(a) shows a bilayer step made by dipping halfway, on a 9/11 layer film of diacetylene monomer deposited on ITO glass. The step height is 5.79 ± 0.09 nm, approximately the length of two molecules. This suggests that the molecules stand perpendicular to the substrate and to the subphase surface, within experimental resolution. Islandlike features with sizes ranging from 14 to 35 nm in diameter are also apparent. The height of these islands, 5.49 ± 0.3 nm, indicates that they are bilayers. rms roughness of the nine-layer film surface in an area of $4 \times 4 \mu\text{m}^2$ is 2.12 nm. This large value in rms roughness is mainly due to the bilayer islands in the film. Between these islands rms roughness in an area of $500 \times 500 \text{ nm}^2$ is 0.68 nm. If the diacetylene molecules have started to collapse locally to form a bilayer, then this could be an intermediate situation with a mixture of bilayer and monolayer on the subphase that survives the film transfer. Hatfield, Taylor, and Bassett [9] have observed this phenomena on both 12-8 and 16-8-diacetylene films. Good molecular resolved images were obtained from these films, and the lattice parameters agree with those obtained from the nine- and 15-layer films above.

Figure 5(b) shows the step of the bilayer of the same film as in Fig. 5(a), but not the same position, after exposing it to uv radiation for 30 min. The film became light red in color, which is a signature of polymerization. The layer thickness determined by the step height decreased to 5.18 ± 0.2 nm and the surface roughness increased to 4.16 nm in the $4 \times 4 \mu\text{m}^2$ area. This large difference in layer thickness indicates that the molecules bend and/or tilt upon polymerization. Similar behavior was observed by Ogawa, Mino, and Tamura [28] in films deposited at high density ($\sim 0.2 \text{ nm}^2/\text{molecule}$). Note that the islandlike features and defects have become much larger in size, which could be resulted due to the bend and/or tilt of the molecules. By counting the number of islands in fixed areas ($500 \times 500 \text{ nm}^2$) at different locations on the sample, we found that the density of islands has increased from $(8.7 \pm 1) \times 10^9/\text{cm}^2$ to $(13 \pm 1.6) \times 10^9/\text{cm}^2$ upon polymerization. Again the reason for this increase in the density of islands could be the bend and/or tilt of the molecules. If there is not enough space parallel to the substrate for the expansion of these islands, then some areas could pop up creating new islands. This enlargement and increase in density of bilayer islands are the reasons for the observed increase surface roughness. Figure 5(c) shows the steps of two separate bilayers deposited on a 9/11/13 layer diacetylene film on ITO glass and subsequent uv polymerization. Step heights are 5.38 ± 0.3 (11/13) and 5.72 ± 0.5 (9/11) nm in agreement with Fig. 5(b). A molecular resolved image of the polymerized film is shown in Fig. 5(d). Average values of lattice parameters obtained from several polymerized samples are slightly larger than those measured before polymerization, and are given in Table I. These values are also slightly larger than those obtained by electron diffraction [7]. As can be seen in this image, periodic height variations are of larger

amplitude in one lattice direction than in the other. This feature was observed in other areas of the film with different tips. The distance between the more pronounced lattice rows is 0.54 ± 0.01 nm and we interpret these rows as the rigid polymer backbones of the film. Gotten *et al.* [26] have shown that upon polymerization of the monomer films there are two possible orientations for the polymer backbone for deposition from the low density phase, and only one orientation for deposition from the high density phase. Our films were transferred to the substrate at a surface pressure of 30 mN/m and $0.2 \text{ nm}^2/\text{molecule}$; thus our monolayers were in the high density phase [28]. In this state diacetylene molecules are arranged in a herringbone pattern [26,28], and only one direction for the polymer backbone is possible upon polymerization. The repeat distance along the polymer backbones of diacetylenes was found to be 0.49 nm [7,30], which is very close to the distance between the periodic height variations along the more pronounced lattice rows in our SFM images of the polymerized sample. Since we operate the SFM in air, the force exerted by the tip on

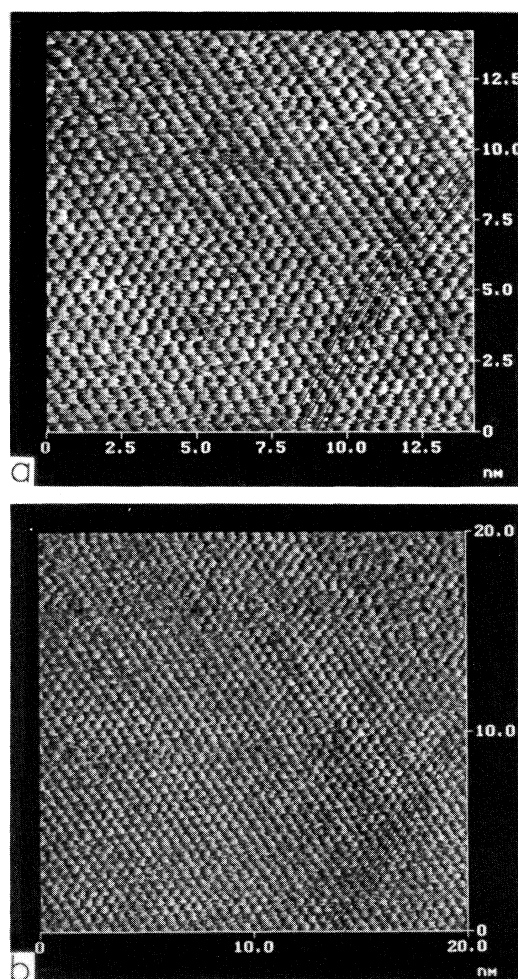


FIG. 6. Two consecutive images in time of a nine-layer film showing the presence of defects. (b) was captured after 47 sec of scanning from the time of capturing (a).

the sample could be strong enough to penetrate through the alkyl chains and resolve the more rigid polymer backbone.

In reality LB films cannot be completely defect free, and in fact we observed different kinds of defects (on both large and small lateral scales) in our diacetylene films. Figures 6(a) and 6(b) show laterally resolved molecular scale defects in one of the samples. These two are unprocessed images and no 3×3 low pass filtering has applied on them. Figure 6(a) was captured initially and after increasing the scanned area to $20 \times 20 \text{ nm}^2$ Fig. 6(b) was captured. The time difference between the two images was 47 sec. The missing row of the molecules at the lower right side of the image is clearly visible in both images. Furthermore, one lattice direction changes, creating a domain boundary. By looking at a glancing angle these defects can be visualized quite well. These types of defects were observed at other sites on the film as well. Ohnesorge and Binnig [19] have reported that to obtain true atomic scale lateral resolution the force exerted on the sample by the SFM tip should be around 10^{-10} N or lower, that scanning in ambient environment gives higher forces, and that this is the reason for largely defect free atomic resolution images reported earlier by SFM. Since we were operating the SFM in air, it was not possible to obtain such low forces. This is because of the large contact area between the tip and the sample due to adhesive forces. Therefore it is possible that the molecular resolved images presented here may be superpositions of several signals or Moiré type imaging of the molecular periodic pattern. However, as pointed out by Todd and Pethica [33], periodicities in these Moiré type images do represent the true molecular periodicities but with large corrugations in the z direction, and with features such as a lack of point defects, blurred nonperiodic features and large corrugations in images which are especially common in layered materials like graphite, where layers can shear parallel to the scanning surface. Recent studies by

Radmacher *et al.* [34] showed that under certain conditions true molecular resolution can be achieved by SFM. They argued that point interaction between the tip and the individual molecules is possible through microroughness of the tip, and that the tip-sample repulsive force is distributed over a large area due to its nonlinear distance dependence. While our images may contain artifacts due to the scanning process, the observation of defects suggests that essential elements of the point structure of these films are being represented in these images.

CONCLUSION

The scanning-force microscope was used to resolve the molecular structure of monomeric and polymeric diacetylene LB films deposited on ordinary microscope and ITO coated glass. Images obtained here indicate that it is not always necessary to have atomically smooth surfaces to obtain molecular resolved images, though the question is still open for monolayer films. uv polymerization decreases the layer thickness by around 10%, and increases the surface roughness as a result of enlargement of bilayer islands. The work reported here confirms that, unlike other techniques such as electron diffraction, x-ray diffraction, etc., SFM gives a real space picture of the lattice and a direct measurement of the lattice parameters. More importantly, SFM alone provides the ability to see the spatial variation of these parameters rather than an average value over a large area, and allows for the observation of defect structures. However, artifacts due to the scanning process must be considered.

ACKNOWLEDGMENTS

This research was supported by the Advanced Liquid Crystalline Optical Materials (ALCOM) program under Grant No. DMR-8920147. We wish to thank Dr. V. Surendranath for his helpful suggestions.

-
- [1] V. K. Agrawal, *Phys. Today* **41** (6), 40 (1988).
 - [2] K. Kjaer, J. Als-Nielsen, C. Helm, P. Tippman-Krayer, and H. Mohwald, *J. Phys. Chem.* **93**, 3200 (1989).
 - [3] Robert F. Fischetti, Mark Filipkowski, Anthony F. Garity, and J. Kent Blasie, *Phys. Rev. B* **37**, 4714 (1988).
 - [4] B. Tieke, G. Lieser, and G. Wegner, *J. Polym. Sci.* **17**, 1631 (1979).
 - [5] A. Fischer and E. Sackmann, *J. Phys. (Paris)* **45**, 517 (1984).
 - [6] S. Garoff, H. W. Deckman, J. H. Dunsmuir, and M. S. Alvarez, *J. Phys. (Paris)* **47**, 710 (1986).
 - [7] Günter Lieser, Bernd Tieke, and Gerhard Wegner, *Thin Solid Films* **68**, 77 (1980).
 - [8] T. Nakanaga, M. Matsumoto, Y. Kawabata, H. Takeo, and C. Matsumura, *Chem. Phys. Lett.* **160**, 129 (1989).
 - [9] J. C. Hatfield, J. W. Taylor, and D. R. Bassett, *Langmuir* **8**, 2976 (1992).
 - [10] Yasushi Tomioka, Shuji Imazeki, and Naoki Tanaka, *Chem. Phys. Lett.* **174**, 433 (1990).
 - [11] G. Binnig, C. F. Quate, and Ch. Gerber, *Phys. Rev. Lett.* **56**, 930 (1986).
 - [12] E. Meyer, L. Howald, R. M. Overney, H. Heinzelmann, J. Formmer, H. J. Güntherodt, T. Wagner, H. Schier, and S. Roth, *Nature* **349**, 398 (1991).
 - [13] D. K. Schwartz, J. Garnaes, R. Viswanathan, S. Chiruvolu, and J. A. N. Zasadzinski, *Phys. Rev. E* **47**, 452 (1993).
 - [14] L. Bourdieu, P. Silberznan, and D. Chatenay, *Phys. Rev. Lett.* **67**, 2029 (1991).
 - [15] R. Kuroda, E. Kishi, A. Yamano, K. Hatanaka, H. Matsuda, K. Eguchi, and T. Nakagiri, *J. Vac. Sci. Technol. B* **9**, 1180 (1991).
 - [16] H. G. Hansma, S. A. C. Gould, P. K. Hansma, H. E. Gaub, M. L. Longo, and J. A. N. Zasadzinski, *Langmuir* **7**, 1051 (1991).
 - [17] R. Guckenberger, B. Hacker, T. Hartmann, T. Scheybani, Z. Wang, W. Wiegräbe, and W. Baumeister, *J. Vac. Sci. Technol. B* **9**, 1227 (1991).
 - [18] Martin Specht, Frank Ohnesorge, and Wolfgang M. Heckl, *Surf. Sci. Lett.* **257**, L653 (1991).
 - [19] F. Ohnesorge and G. Binnig, *Science* **260**, 1451 (1993).

- [20] H. E. Gaub (unpublished).
- [21] Kazufumi Ogawa, Norishisa Mino, Hideharu Tamura, and Nobuo Sonoda, *Langmuir* **5**, 1415 (1989).
- [22] D. Bloor, D. J. Ando, F. H. Preston, and G. C. Stevens, *Chem. Phys. Lett.* **24**, 407 (1974).
- [23] L. F. Chi, L. M. Eng, K. Graf, and H. Fuchs, *Langmuir* **8**, 2255 (1992).
- [24] Constant A. J. Putman, Helen G. Hansma, Hermann E. Gaub, and Paul K. Hansma, *Langmuir* **8**, 3014 (1992).
- [25] Troy E. Wilson, D. Frank Ogletree, Miquel B. Salmeron, and Mark D. Bednarski, *Langmuir* **8**, 2588 (1992).
- [26] Babara M. Goettgens, Ralf W. Tillmann, Manfred Radmacher, and Hermann E. Gaub, *Langmuir* **8**, 1768 (1992).
- [27] H. D. Göbel, H. E. Gaub, and H. Möhwald, *Chem. Phys. Lett.* **138**, 441 (1987).
- [28] Kazufumi Ogawa, Norihisa Mino, and Hideharu Tamura, *Jpn. J. Appl. Phys.* **28**, 2314 (1989).
- [29] David Day and J. B. Lando, *Macromolecules* **13**, 1478 (1980).
- [30] David Day and J. B. Lando, *Macromolecules* **13**, 1483 (1980).
- [31] S. P. Walsh, Ph.D. dissertation, Case Western Reserve University, 1992; S. P. Walsh and J. B. Lando, *Langmuir* **10**, 246 (1994).
- [32] M. Radmacher, B. M. Goettgens, R. W. Tillmann, H. G. Hansma, P. K. Hansma, and H. E. Gaub, in *Scanned Probe Microscopy*, edited by H. K. Wickramasinghe, AIP Conf. Proc. No. 241 (AIP, New York, 1991), p. 144.
- [33] J. D. Todd and J. B. Pethica, *J. Phys. Condens. Matter* **1**, 9823 (1989).
- [34] M. Radmacher, R. W. Tillmann, M. Fritz, and H. E. Gaub, *Science* **257**, 1900 (1992).

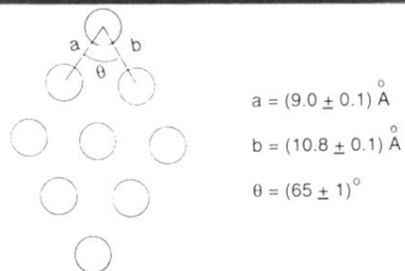
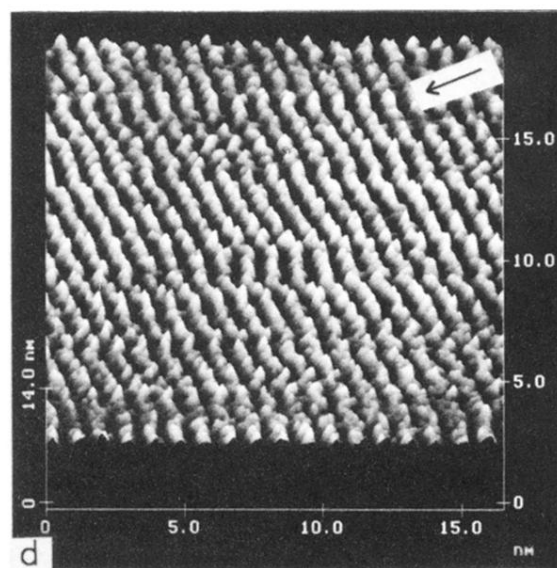
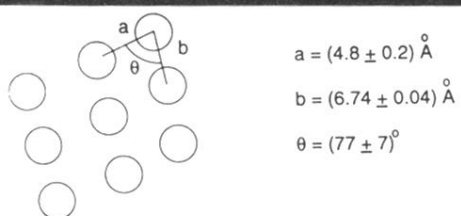
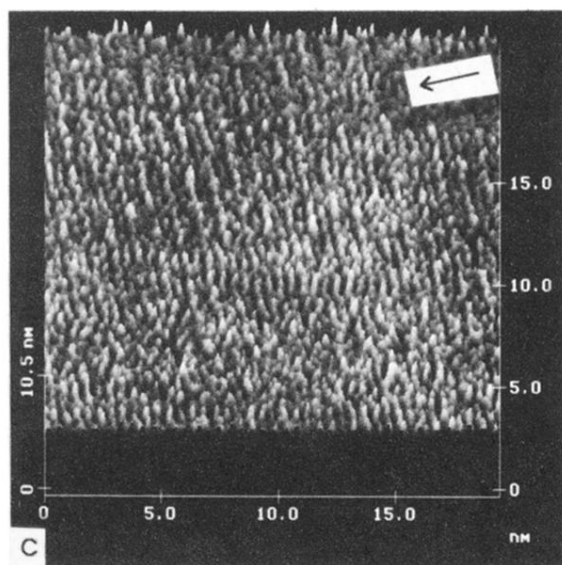
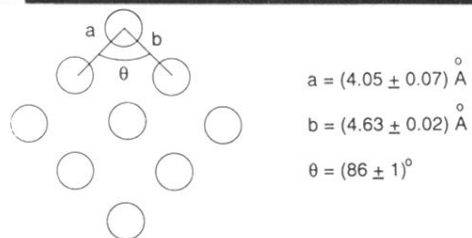
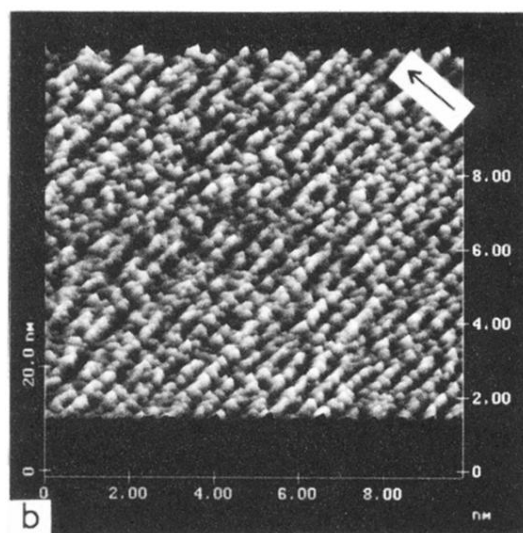
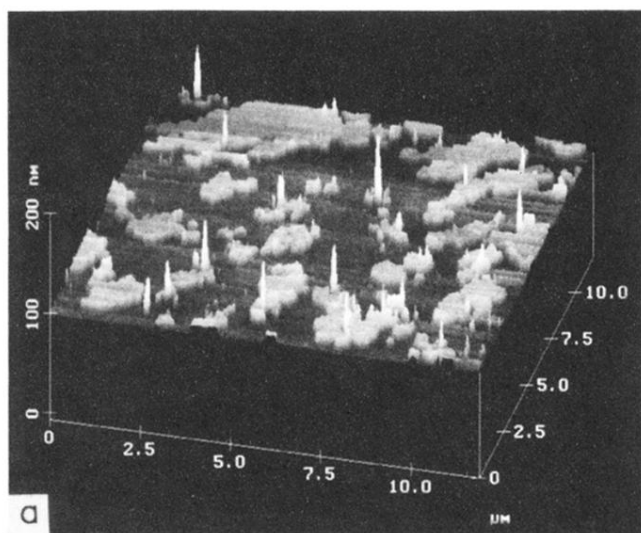
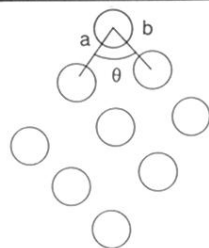
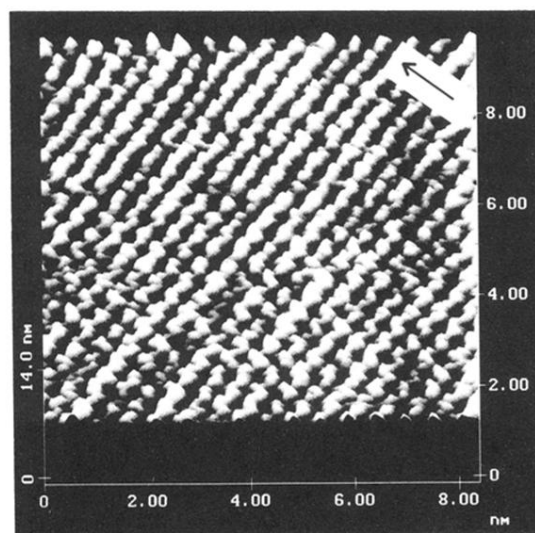


FIG. 2. (a) $12 \times 12\text{-}\mu\text{m}^2$ SFM image of the surface obtained after completion of one cycle through the diacetylene monolayer. (b)–(d) Molecular-resolved SFM images with the lattice structures obtained on three different islands. Arrow indicates the direction of dipping.

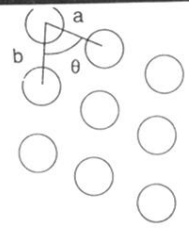
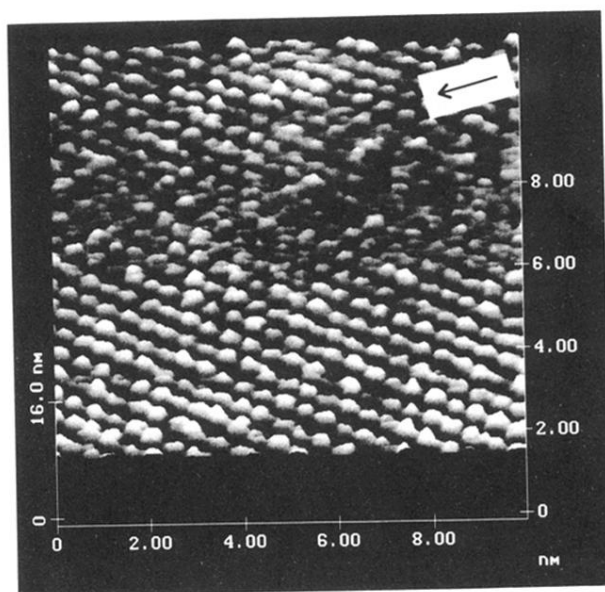


$$a = (4.34 \pm 0.02) \text{ \AA}$$

$$b = (4.49 \pm 0.05) \text{ \AA}$$

$$\theta = (76 \pm 1)^\circ$$

FIG. 3. Image with molecular resolution of a nine-layer film with the lattice structure. The arrow indicates the direction of dipping.



$$a = (4.65 \pm 0.08) \text{ \AA}$$

$$b = (4.81 \pm 0.03) \text{ \AA}$$

$$\theta = (71 \pm 2)^\circ$$

FIG. 4. Image with molecular resolution of a 15-layer film with the lattice structure. The arrow indicates the direction of dipping.

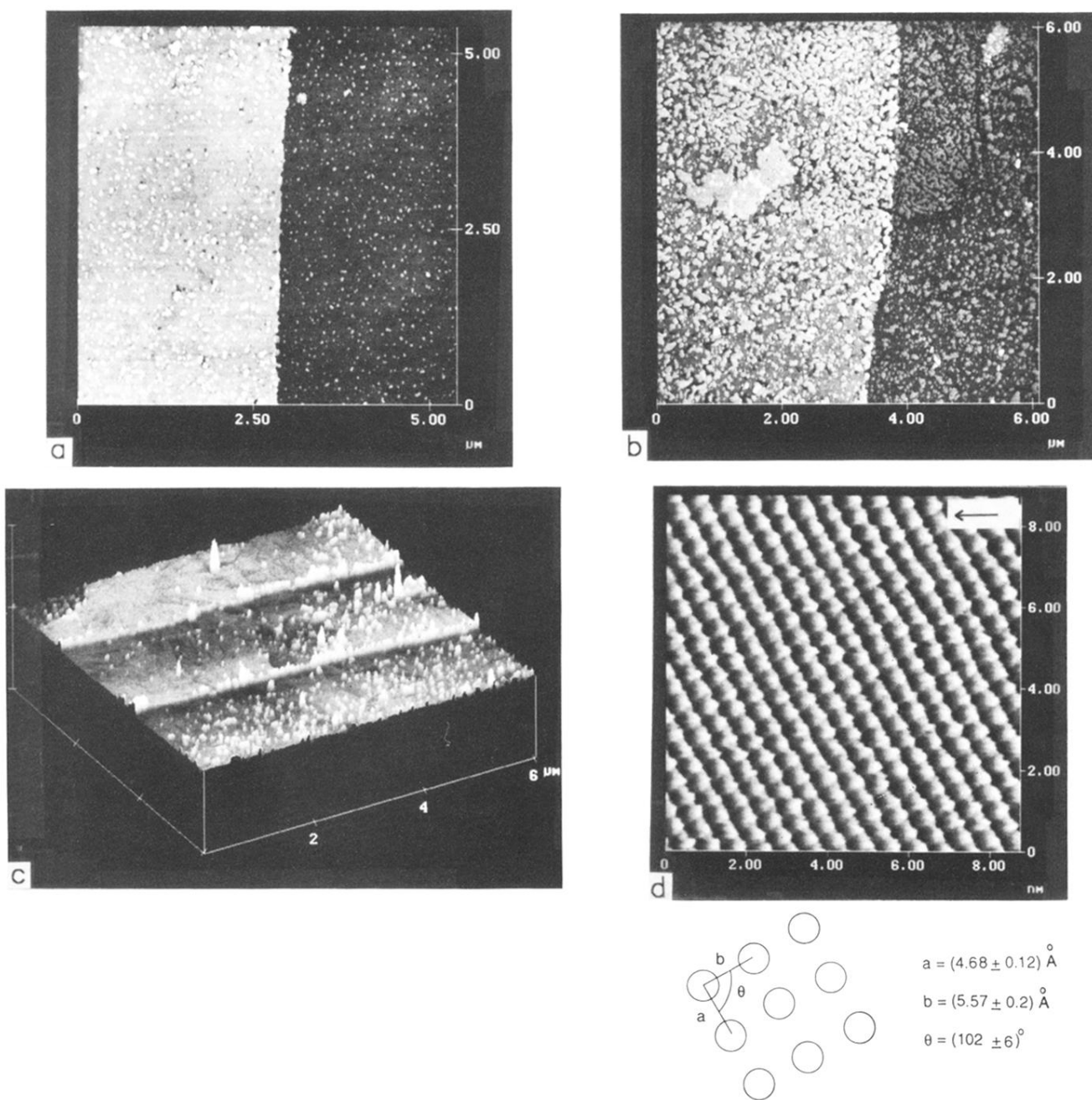


FIG. 5. (a) Image of a bilayer step deposited on a 9/11 layer film on ITO glass. (b) Image of the different position of the same step as in (a) after exposure to uv radiation for 30 min. (c) Image of three bilayer steps; 9/11/13 layers deposited on ITO glass. (d) $12.5 \times 12.5\text{-nm}^2$ image with molecular resolution of a nine-layer polymerized film with the lattice structure. The arrow indicates the direction of dipping.

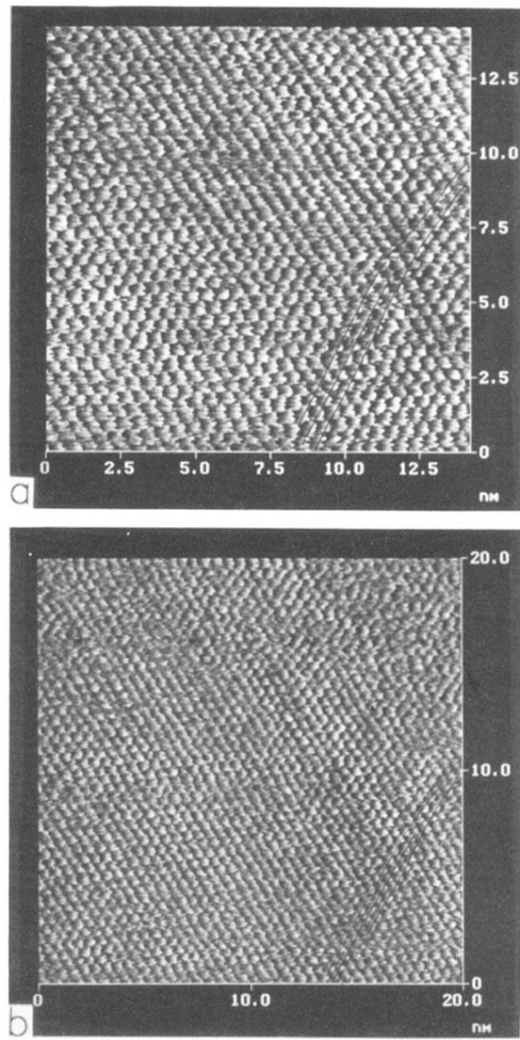


FIG. 6. Two consecutive images in time of a nine-layer film showing the presence of defects. (b) was captured after 47 sec of scanning from the time of capturing (a).